Ali *et al.*
Journal of Engineering and Applied Science (2022) 69:38
https://doi.org/10.1186/s44147-022-00093-5

Journal of Engineering and Applied Science

RESEARCH Open Access

Design and structural analysis of non-pneumatic tyres for different structures of polyurethane spokes

Muhammad Ali*, Muhammad Maarij and Azhar Hussain

*Correspondence:
mali68347@gmail.com
Department of Mechanical Engineering, Faculty of Mechanical & Aeronautical Engineering, University of Engineering and Technology, Taxila, Pakistan

Abstract

NPTs have vast applications because of no tyre puncture, no need for air pressure, low rolling resistance, and also have higher flexibility for design and recyclability. In this research work, different structures of polyurethane (PU) spokes have been designed and analyzed under radial loading conditions which include structures like honeycomb with varying cell angles, simple spoke, and trapezoid type by keeping in view that the cell wall thickness and somehow the mass of the structures remain the same. Based on the Mooney-Rivlin hyper-elastic material model and performing 2D non-linear static structural analysis on different types of NPTs using ANSYS, it has been observed that the simple spoke structure has the lowest spoke stress and deformation values of 2.01 MPa and 11.7 mm, while HC–A1 has the least value of strain energy of 2.58 mJ, at a load of 2500 N. The above results show that the straight spoke structures like simple spoke and trapezoid type have a high load-carrying ability than the honeycomb type NPTs under same boundary conditions. While honeycomb NPTs have higher fatigue life as compared to straight-spoke NPTs.

Keywords: Non-pneumatic tyre (NPT), Polyurethane (PU), Spokes, Contact pressure, Deformation, Stress, Mooney-Rivlin (MR), ANSYS, Structural analysis

Introduction

Since the invention of non-pneumatic tyre (NPTs) in the 1920s, they are getting more recognition over their pneumatic counterpart because of their advantages such as low rolling resistance, no flat tyres, and no need for air pressure maintenance [1, 2]. An NPT is made up of a hub, flexible number of spokes, a tread, and a shear ring. The tread part is made of synthetic rubber, and the shear ring portion is made of two components one is the shear band and the other includes two inner and outer steel rings. The flexible portion of the NPT consists of polyurethane material spokes that connect to the hub and shear composite ring of NPT and are deformed mainly by tension, buckling, compression, and bending during the rolling of tyre. Because of such deformations, it is necessary to minimize the stresses in spokes during driving. So, such a design needs to be given importance which has high fatigue resistance.

The NPT spokes must have a high value of resilience and stiffness under the loading conditions of compression or tension. The honeycomb spokes have a high value of strength and stiffness in normal to the plane directions, and in the in-plane coordinate or direction, they have a higher resilience value and lower value of mechanical resistance [3]. The honeycomb cell structures are also changeable to optimize the in-plane and out-plane properties of spokes that is by changing the inside angles of the honeycomb spokes, as well as the length and thickness of the wall of spokes to get variable strength and stiffness values [4, 5]. Honeycomb hexagonal spoke structures have been utilized in many applications, and also for the design of delicate component structures. In recent years, some in-plane structures yield strength values, their modulus of elasticities, and also their buckling behaviors, of various cell types including straight, triangular, hexagonal, diamond, and square ones have been studied [6–8].

Kim [9] has studied the structural analysis of NPTs with honeycomb spokes by applying vertical loads and found that, because of the high stiffness of NPT spokes, the contact pressure values of NPTs were lower than that of a pneumatic tyre. Ju et al. [10] compared spokes of hexagonal auxetic honeycombs with conventional honeycomb spokes and it was concluded that under the same load-carrying capacity the conventional honeycomb spokes which had a highly positive cell spoke angle had low values of mass and also low local stresses.

Methods

Methodology

The methodology is composed of deep literature research from previous work on pneumatic and NPTs to design and analyze new polyurethane spoke structures according to standard (GBT 2977-2008) which have least amount of deformation, stress, and strain energy values. The material properties of all the metallic parts of the tyre were taken from previous research work including the non-linear material data of polyurethane and synthetic rubber [11]. A honeycomb NPT (NPT-A1) [12] was taken as a standard design to set the boundary and mesh parameters in ANSYS and compare the results of the stress analysis of HC-A1 based on Mooney-Rivlin (MR) hyper-elastic material model, with the previous research of NPT-A1, by applying a point load at the center of the aluminum hub. After the stress results of HC-A1 matched with the stress results of NPT-A1 with minimum error, then the same boundary and mesh parameters were used for the newly designed spoke structures. The newly designed NPTs spoke structures dimensions were also designed as per standard (GBT 2977-2008) and only the designs of spoke structures were changed by keeping the mass of the spoke structures almost constant. These include the three positive cell angle honeycombs (HC-A1, HC-A2, and HC-A3), simple straight spoke type, and trapezoid type NPTs spoke structures. In this paper, the non-linear static structural analysis of NPTs with different spoke structures was numerically analyzed and simulated. The deformation modes, stress distribution in treads and spokes, and the strain energy parameters of different designs of NPTs were studied thoroughly.

Properties

Geometric parameters

Two dimensional (2D) models for the finite element analysis (FEA) were modeled on SolidWorks software and then numerically solved on ANSYS software. As shown in Fig. 1, an NPT consists of a rubber tread, two steel rings, a polyurethane shear band, several polyurethane spokes, and a central aluminum alloy hub. The NPT width and the outermost diameter were designed equal to 215 mm and 664 mm, according to the Chinese truck tyre standard, GBT 2977-2008. The earlier honeycomb engineers developed the effective in-plane moduli of hexagonal honeycombs using the beam theory, and these developments are called cellular materials theory (CMT) [10]. The honeycomb spoke structures in-plane elastic modulus values were determined in the previous articles as per CMT which are also given below [13–15]:

$$E_r^* = \frac{E_s\left(\frac{a}{l}\right)^3 cos\theta}{\left(\frac{h}{l} + sin\theta\right)\sin^2\theta} \tag{1}$$

$$E_{\cap}^* = \frac{E_s\left(\frac{a}{l}\right)^3\left(\frac{h}{l} + sin\theta\right)}{\cos^2\theta} \tag{2}$$

$$G_{r\cap}^* = \frac{E_s\left(\frac{a}{l}\right)^3\left(\frac{h}{l} + sin\theta\right)}{\left(\frac{h}{l}\right)^2(1 + 2h/l)\cos\theta} \tag{3}$$

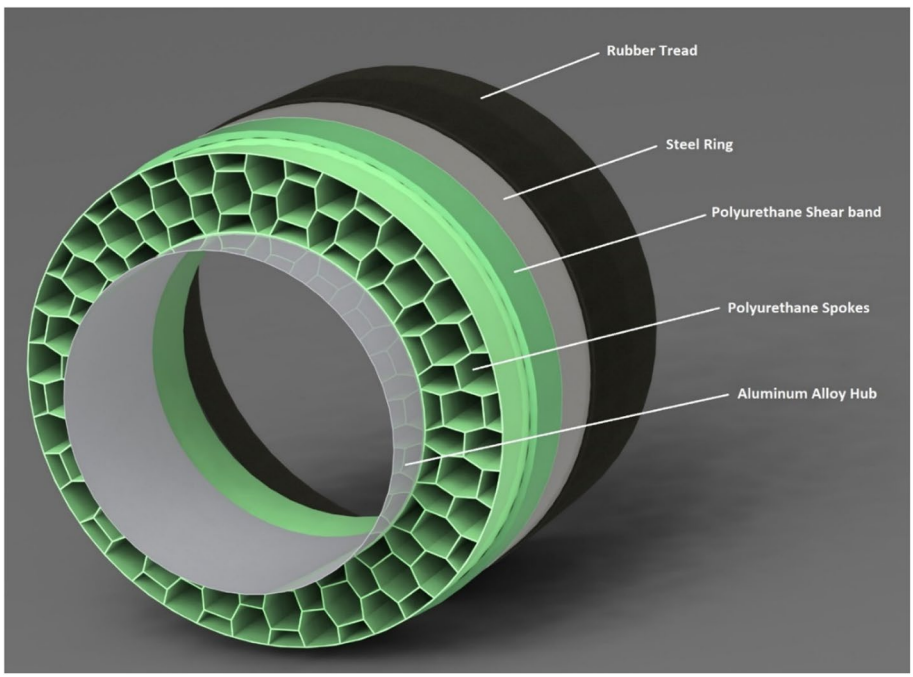

Fig. 1 Photo of NPT with all the components including honeycomb spokes

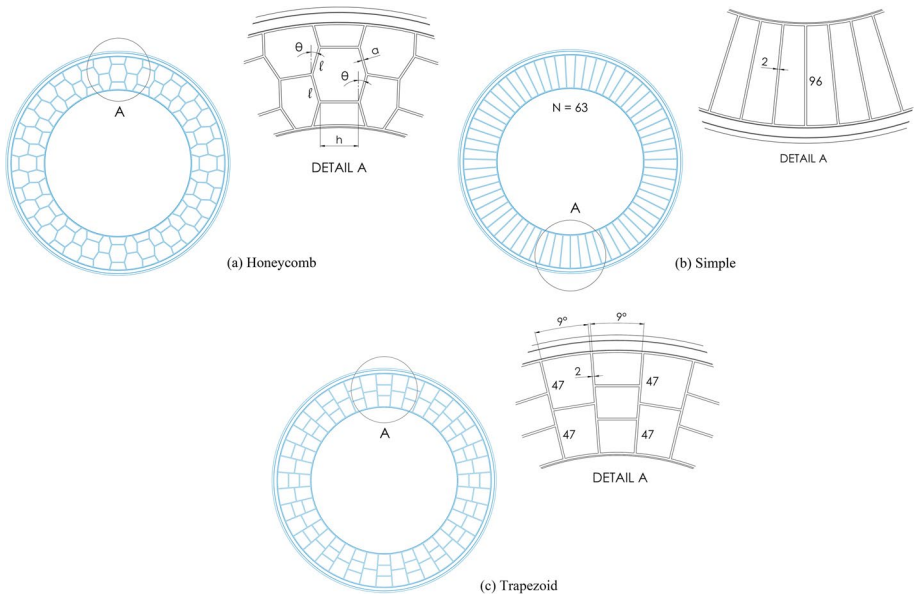

Fig. 2 Geometrical and schematic pictures of spoke cells

where E_r^*, $E_{\cap}^*$, and $G_{r\cap}^*$ are the effective modulus values in the radial, circumferential, and shear directions. As shown in Fig. 2a, the θ, l and h represent the values of the spokes cell angle, cell inclined length, and vertical length of the cell. The 'a' represents the cell wall thickness as shown in Fig. 2 and E_s represents the value of the base material's young modulus.

Now to obtain the density of the honeycomb structure, we can use the below formula [12]:

$$\rho^* = \frac{\rho_s\left(\frac{a}{l}\right)\left(\frac{h}{l}+2\right)}{2\cos\theta\left(\frac{h}{l}+sin\theta\right)} \tag{4}$$

Where the base material density value is denoted by $\rho_s = 1200$ kg/m^3 [10, 16]. As a basic part of an NPT, the ratio between the height and cell inclined length in the spokes of honeycomb is an important variable just to design the out-plane and in-plane structures of flexible spokes under different loading conditions [10]. This is clearly shown by changing the honeycomb's cell angles. In this research work, three different unique honeycombs have been designed including 15.76°, 12°, and 7° cell angles, θ. The HC-A2 and HC-A3 are new designs of NPTs having a unique cell angle of 12° and 7° respectively. Now the reason for choosing the different values of cell angles θ is because a high cell angle causes the honeycomb spoke structures to have more flexibility under uni-axial loading than the low cell angle spoke structures that have a low amount of flexibility [10]. Also, two new designs of straight spoke structures have been designed as well named simple spoke and trapezoid spoke based NPTs.

The cell wall thickness 'a' for all the spoke designs are set equal to 2 mm and the mass values of all the different spoke structures have been made almost equal with some small variations. All the geometrical and other properties of different honeycomb spoke structures are given in Table 1, and their models are shown in Fig. 3.

Table 1 Honeycomb (HC) spokes mechanical and geometrical properties

Type	*l* (*mm*)	*h* (*mm*)	*θ* (°)	ρ^*/ρ_s	E_r/E_s	$E^*_{r\cap}/E_s$	$G^*_{r\cap}/E_s$
HC-A1	26.25	36.66	15.76	0.08	3.46×10^{-3}	8.14×10^{-4}	1.03×10^{-4}
HC-A2	25.56	36.38	12	0.08	6.64×10^{-3}	8.17×10^{-4}	1.025×10^{-4}
HC-A3	25.19	39.23	7	0.08	0.02	8.5×10^{-4}	8.5×10^{-5}

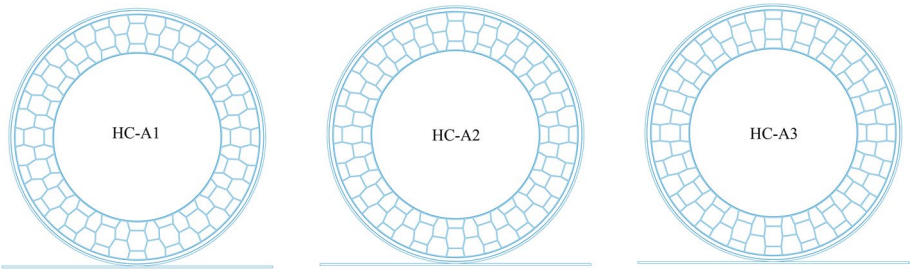

Fig. 3 Honeycomb spokes-based NPTs with the same wall thickness with different cell angles

The simple spoke type NPT has the length of each spoke equally to 96 mm and the total number of spokes (N) divided at an equal angle, is 63 as shown in Fig. 2b. The trapezoid spoke type NPT has an angle value of 9° between the two spokes and the vertical spoke is divided into parts each having a length of 47 mm as shown in Fig. 2c.

Material properties

The aluminum alloy 7075-T6, steel alloy ANSI 4340, synthetic rubber, and polyurethane material properties were used for the hub, two steel rings, tread, and shear bands for all parts of NPTs [11]. Polyurethane and synthetic rubber are non-linear hyper-elastic materials and in ANSYS software these materials were modeled using the Mooney-Rivlin (MR) theory [17]. The mass value of all different types of polyurethane spokes was set almost equal with some small variations as shown in Table 2 [10, 16]. The material models of MR for non-linear materials use strain energy (W) equations as a function to calculate other variables. The strain energy (W) function can be written in the equation form while not taking into account the temperature and volumetric deformation changing terms [17, 18]. These values were neglected just to make the numerical problem simple and as this is a pure non-linear structural stress analysis so temperature effects were ignored and were left for future study purposes.

Table 2 Mass values of different polyurethane spoke structures [10, 16]

Sr. No.	Spoke structure	Mass (g)
1.	HC-A1	4857.28
2.	HC-A2	4856.24
3.	HC-A3	4902.96
4.	Simple spoke type	4852.08
5.	Trapezoid spoke type	4950.56

$$W = \sum_{i+j=1}^{n} C_{ij}(I_1 - 3)^i (I_2 - 3)^j \tag{5}$$

The invariants of the deformation are denoted by I_1, I_2 and material constants are denoted by the term, C_{ij}. The invariants of the deformation are written below:

$$I_1 = \lambda_1^2 + \lambda_2^2 + \lambda_3^2 \tag{6}$$

$$I_2 = \lambda_1^2\lambda_2^2 + \lambda_2^2\lambda_3^2 + \lambda_3^2\lambda_1^2 \tag{7}$$

The elongations along the different axis of the element are denoted by the terms $\lambda_1, \lambda_2, \lambda_3$. The ANSYS software has the availability of using all the different models of MR equations based on the different C_{ij} constants including the 2, 3, 5, and 9 parameters where, $i=1$, 2, 3, 4, 5, ….9 and $j=1$, 2, 3, 4, 5, ….9. In this research work, the MR 9 parameter material model was used in ANSYS. The uniaxial, biaxial, and planar shear experimental test data was available in a recent research work [11]; that data was used in this research work to calculate the stresses and deformation values in different spokes. Some of the basic modes of deformation and their relationships with other elongations are shown in Fig. 4 [17].

Assuming that the material is incompressible then:

$$\lambda_1^2\,\lambda_2^2\lambda_3^2 = 1 \tag{8}$$

Now taking, $\lambda = 1 + \varepsilon$, where ε is the engineering strain of the sample and putting this value in the above Eqs. 6 and 7, then the different deformation modes can be written as follows [17]:

- The deformation mode for the uniaxial term

$$I_1 = \lambda^2 + 2\lambda^{-1} \qquad I_2 = 2\lambda + \lambda^{-2} \tag{9}$$

- The deformation mode for the biaxial term

$$I_1 = 2\lambda^2 + \lambda^{-4} \qquad I_2 = \lambda^4 + 2\lambda^{-2} \tag{10}$$

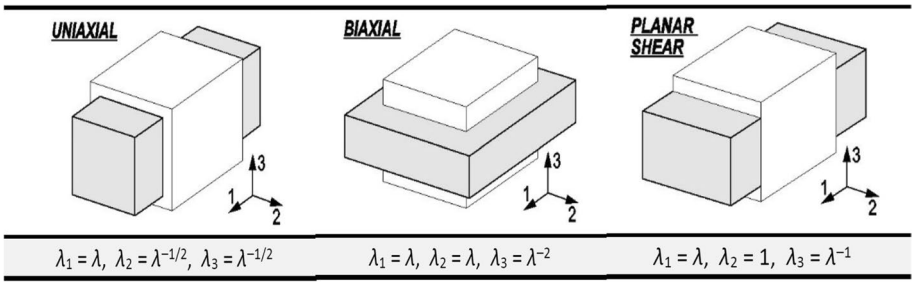

Fig. 4 Uniaxial, biaxial, and planar shear deformation modes and relationships between the elongations

- The deformation mode for the planar shear term

$$I_1 = \lambda^2 + \lambda^{-2} \qquad I_2 = \lambda^2 + \lambda^{-2} \tag{11}$$

Since the strain energy (W) has been defined, we can determine the values of the stresses along with the different directions as a derivative, $\sigma(\varepsilon) = \partial W/\partial\varepsilon$, where ε is the strain value and σ is the stress value. For all of the MR models, the strain energy (W) terms were converted to such a form which had the elongations λ along with different directions as well as the C_{ij} constant terms. The MR second order, third order $\sigma(\lambda)$, and ninth order $W_{(9)}$ (strain energy-based) relations for only the uniaxial deformation modes are shown below:

1. Mooney-Rivlin 2 parameter model

$$\sigma(\lambda) = 2\left[C_{10}\left(\lambda - \lambda^{-2}\right) + C_{01}\left(1 - \lambda^{-3}\right)\right] \tag{12}$$

2. Mooney-Rivlin 3 parameter model

$$\sigma(\lambda) = 2\left[C_{10}\left(\lambda - \lambda^{-2}\right) + C_{01}\left(1 - \lambda^{-3}\right) + 3C_{11}\left(\lambda^2 - \lambda - 1 + \lambda^{-2} + \lambda^{-3} - \lambda^{-4}\right)\right] \tag{13}$$

3. Mooney-Rivlin 9 parameter model

$$\begin{aligned} W_{(9)} = {} & C_{10}\left(\overline{I}_1 - 1\right) + C_{01}\left(\overline{I}_2 - 1\right) + C_{20}\left(\overline{I}_1 - 1\right)^2 + C_{02}\left(\overline{I}_2 - 1\right)^2 \\ & + C_{11}\left(\overline{I}_1 - 1\right)\left(\overline{I}_2 - 1\right) + C_{30}\left(\overline{I}_2 - 1\right)^2 + C_{03}\left(\overline{I}_2 - 1\right)^3 \\ & + C_{21}\left(\overline{I}_1 - 1\right)^2\left(\overline{I}_2 - 1\right) + C_{12}\left(\overline{I}_1 - 1\right)\left(\overline{I}_2 - 1\right) + \frac{1}{d}(J-1)^2 \end{aligned} \tag{14}$$

The C_{ij} constant terms can be found out by using the stress-strain data that is obtained from the compression/tension experimental test data for the polyurethane and synthetic rubber hyper-elastic materials from the previous research work [11]. In this research work, the C_{ij} terms were found in ANSYS using the data fitting algorithm, that is solved using the least squares method. Figures 7 and 8 show the curve fit material models solved using ANSYS MR 9 parameter model, for polyurethane and synthetic rubber materials based on the experimental test data from previous research work [11]. From Figs. 5 and 6, the theoretical data curves calculated using ANSYS MR 9 parameter model fits perfectly with the experimental material test data points, so we have used the MR 9 parameter model for our analysis purpose. So, this validates that the material constants calculated for polyurethane and synthetic rubber materials using MR 9 parameter model are accurate.

Numerical methodologies

A 2D analysis type geometry option is set in ANSYS and the NPT width value is set equal to 215 mm (according to the Chinese GBT 2977-2008 standard). A rigid point load was added at the center of the aluminum alloy hub and its value is ranged from 500 to

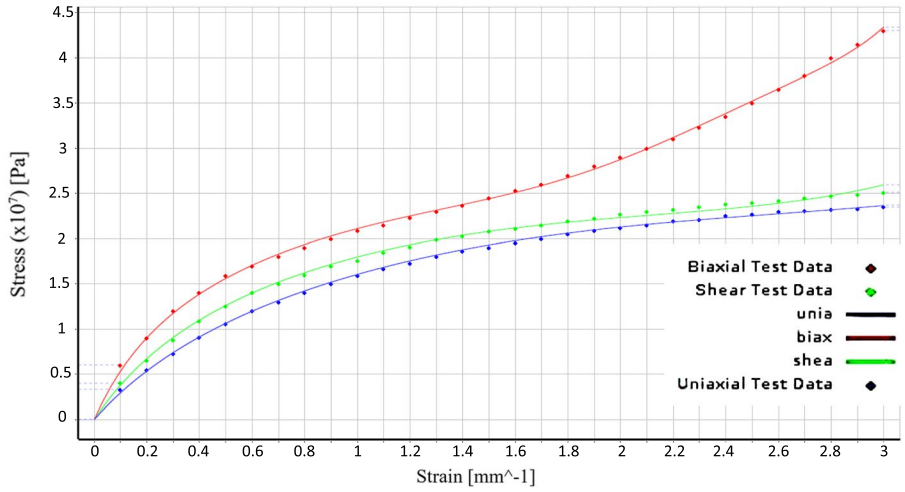

Fig. 5 Polyurethane material model for all deformation modes (uniaxial, biaxial, and shear test data) using MR 9 parameter model to evaluate the C_{ij} constants

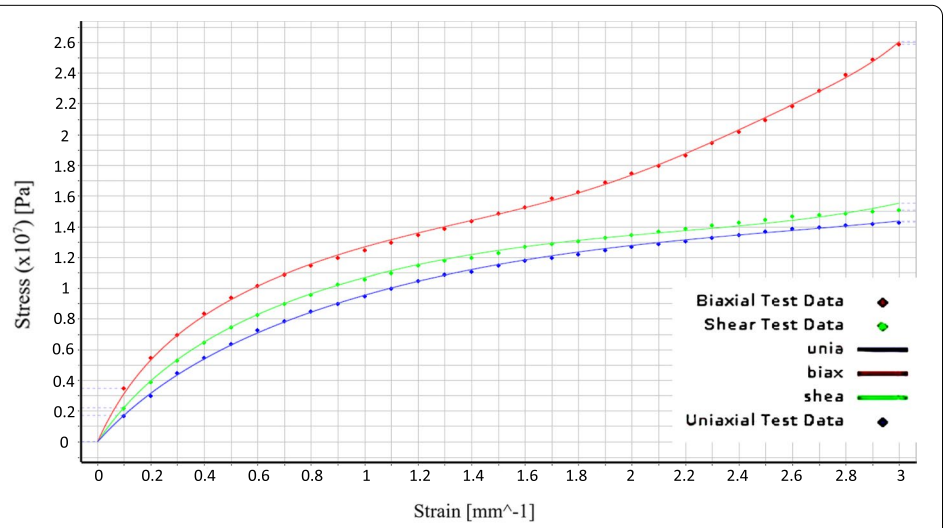

Fig. 6 Synthetic rubber material model for all deformation modes (uniaxial, biaxial, and shear test data) using MR 9 parameter model to evaluate the C_{ij} constants

2500 N, as per the load-carrying capacity of the NPT according to standard (GBT 2977-2008) [12]. The simulation method in this regard is important and requires a few considerations to be analyzed before the numerical methods. It is important to understand that the physical bodies are only in contact with each other instead of inter-penetrating. Therefore, the software solution will require the prior setting of the program in such a way that the relationship between contact surfaces is established.

In the details of the connections, manual contact regions were established between the 2D parts of the NPT assembly which included the bonded and frictional type contact regions. The bonded and frictional type contact was established between the internal peripheries of the different geometries and between the outer edge of the tread and the flat platform on which the whole NPT is placed. A friction coefficient

value was set equal to 0.15, which is normally used to avoid the slipping conditions during the analysis [12]. A point contact is established between the tread and the flat platform and the mesh was refined around that contact area so to overcome the convergence issues that occur when changing the load values on the hub, advanced contact options can also be used. The physical bodies in contact do not interpenetrate. Therefore, the simulation program must establish a relationship between the two contact surfaces to prevent the two contact bodies from penetrating into each other in the simulation as shown in Fig. 7.

ANSYS provides different contact algorithms to enforce contact compatibility at the interface. In the advanced contact options, the first thing to consider is the formulation option which includes the Augmented Lagrange and Pure Penalty contact algorithms. For the nonlinear simulations and body contacts, the most used formulations are Pure Penalty and Augmented Lagrange, normally both are penalty-based contact methods [19].

$$F_{\text{normal}} = k_{\text{normal}} x_{\text{penetration}} \tag{15}$$

F_{normal} is the normal contact force, k_{normal} is the contact stiffness value so when the contact stiffness is high then the penetration, $x_{\text{penetration}}$ value is low. In an ideal case when the k_{normal} value is infinite, then there would be zero penetration between the bodies. The default value of stiffness is automatically determined by ANSYS. For bulk dominated analysis one can use, $k_{\text{normal}} = 1$ and for bending dominated problems one can use $k_{\text{normal}} = 0.01$ *to* 1. With penalty-based methods, this is not numerically possible but as long as the $x_{\text{penetration}}$ value is negligible or small, then the solution results will be accurate. For the Augmented Lagrange method, the equation used is given below [19]:

$$F_{\text{normal}} = k_{\text{normal}} x_{\text{penetration}} + \lambda \tag{16}$$

The Augmented Lagrange method is less delicate to k_{normal} contact stiffness extent because of the λ term in the above equation. Contact penetration is present in the Augmented Lagrange method but can be controlled to some degree. The main difference between Pure Penalty and Augmented Lagrange methods is that the latter augments the

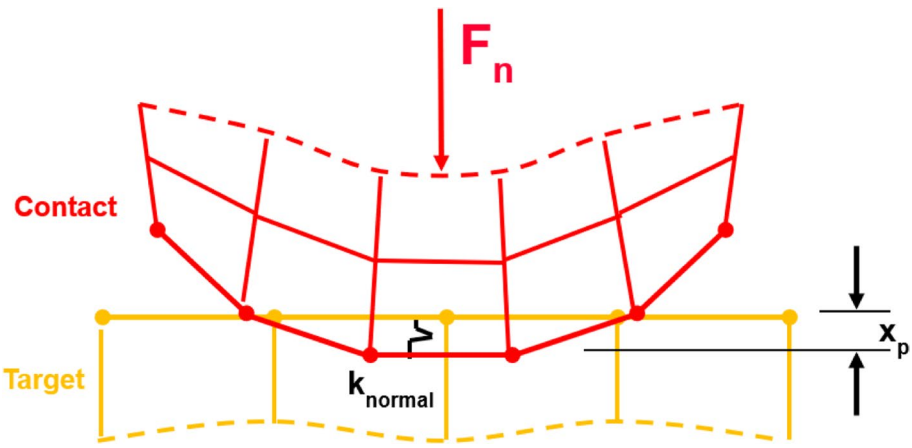

Fig. 7 Relation between normal force, contact stiffness, and contact penetration [19]

contact force (pressure) calculations. The k_{normal} stiffness value is a very important variable that affects both the convergence phenomenon as well as the accuracy of the analysis. When we use large values of stiffness, k_{normal} the accuracy of the analysis is increased but the analysis may have some difficulties in converging the solution.

Now for the boundary conditions, fix support was applied to the flat platform part of the NPT assembly. A standard Earth gravity was applied to all the parts of the NPT in the negative Y-axis direction whose value was set equal to $-9.8066\ \text{ms}^{-2}$.

In the mesh section quadrilateral, dominant mesh method and quadrilateral/triangular mixed mesh elements were used for all the parts of the NPT assembly. Element size of 0.5 mm was set for the tread, two steel rings, hub, and the flat platform of NPT. While element size of 1 mm was set for the spokes and the shear band of NPT. A point contact is set between the tread and the flat platform, so to avoid the convergence errors in the analysis, the mesh was refined around the contact region by setting the element size equal to 0.2 mm and the sphere radius equal to 15 mm. Refined meshing around the point contact region is shown in Fig. 8 for HC-A1 NPT.

Skewness term is defined as the difference between the shape of the equilateral cell and the shape of the cell of an equivalent volume. If the cells are highly skewed, then the solution accuracy is decreased and destabilized. Orthogonal quality is computed with vector mechanics. Calculations are done by using the face normal vector, the vector from the cell centroid to the centroid of each of the adjacent cells, and the

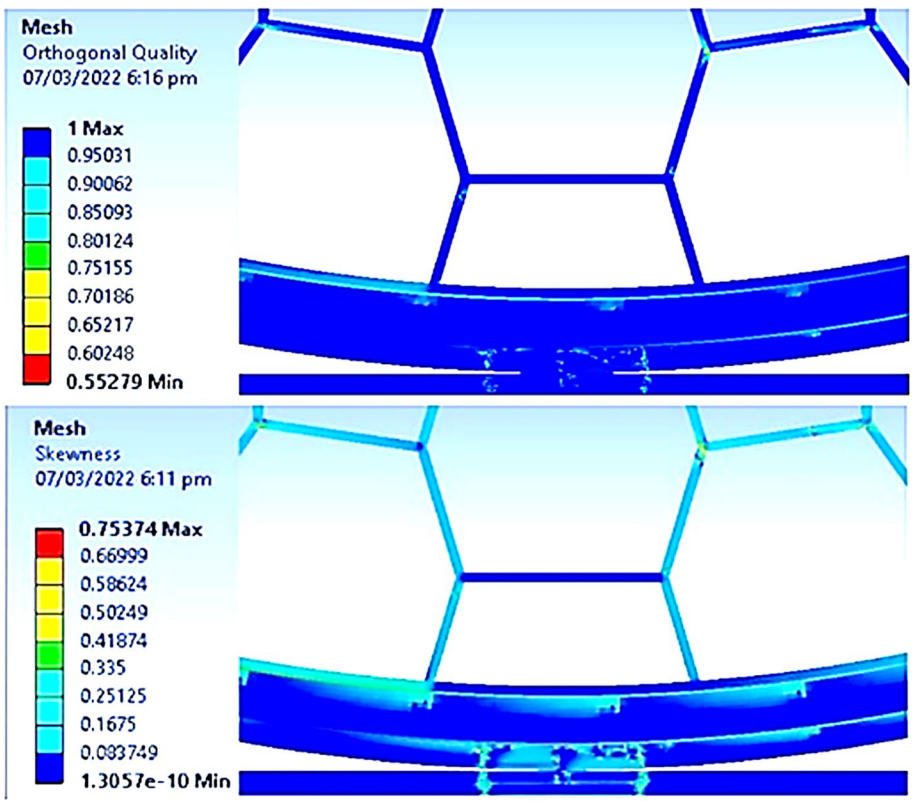

Fig. 8 Refined meshing around the point contact region showing the orthogonal and skewness mesh quality

vector from the cell centroid to each of the faces. The skewness values ranging from 0.25 to 0.8 are acceptable and the orthogonal quality values ranging from 0.2 to 1.0 are also acceptable [20]. The above mesh parameters were finalized after doing the mesh convergence analysis on the HC-A1 type spokes. A point load of 2000 N was applied at the center of the hub of NPT assembly. In the mesh convergence analysis, different element sizes were changed accordingly to obtain the total number of mesh elements. The NPT model was simulated to obtain the value of maximum stress in the polyurethane spokes and that value was plotted against the total number of elements. Table 3 shows the number of elements, skewness and the orthogonal quality of meshing, and the amount of maximum stress obtained after analyzing HC-A1 NPT. Figure 9 shows the mesh convergence plots for all types of NPTs used in this research work.

The percentage of error for maximum stress (MPa) between 1.93 and 1.96 is equal to 1.53% for HC-A1 NPT. So, the properties of mesh that were used for the maximum stress of 1.93 MPa were finally set for all the structures of NPT assemblies to get the final results. A higher number of mesh elements settings can also be used but it would require a lot of computing power and time to solve the analysis. So, from the above mesh analysis, it is validated that the mesh quality and mesh parameters are correct.

Table 3 Number of elements and nodes, skewness, orthogonal quality, and maximum stress values for mesh convergence analysis of HC-A1 NPT

Sr. No.	Number of elements	Number of nodes	Stress in spokes (MPa)	Skewness	Orthogonal quality
01	53868	199383	1.56	0.8071	0.4467
02	113417	395570	1.57	0.8071	0.6
03	**216079**	**743722**	**1.93**	**0.7537**	**0.5528**
04	271473	913934	1.96	0.7537	0.5528
05	492808	1585961	1.94	0.7537	0.5528

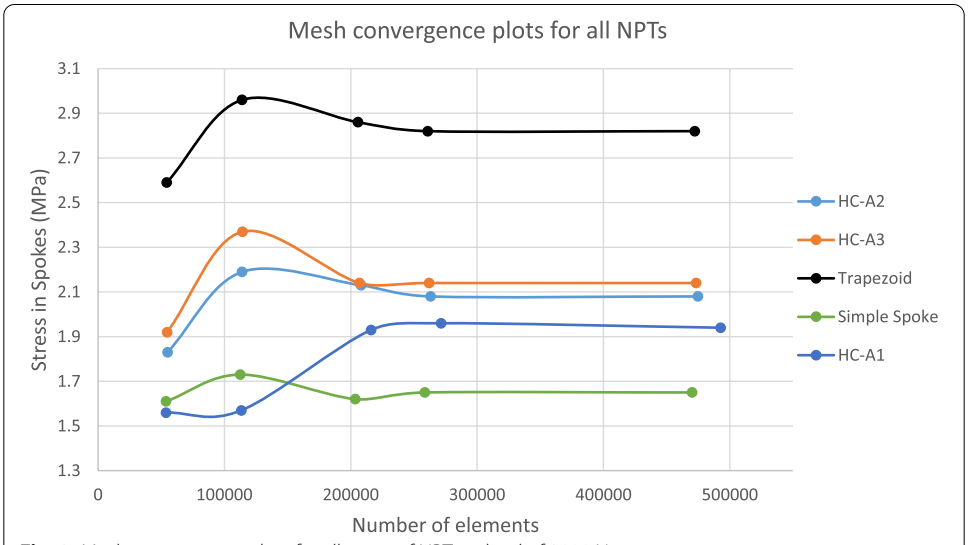

Fig. 9 Mesh convergence plots for all types of NPTs at load of 2000 N

Results and discussion

Vertical loads results among the NPTs

In the analysis of NPTs, all the spoke structures were designed in such a way so that mass of the NPT structures was almost kept equal to each other. The mesh properties were kept the same as of HC-A1 for all the other NPT structures in the analysis. Five types of NPT static behavior were thoroughly investigated by applying vertical static loads ranging from 500 to 2500 N. Table 4 shows the results of all types of NPTs under the vertical force/load. The stress in the spokes and treads, deformation behavior of spokes, and strain energy behavior in the spokes of NPTs were investigated and were compared with each other to choose the one which had the least amount of deformations and stress values. The results with brief discussion are given below for all the NPTs including the analysis contours with results graphs.

As per the analysis, our main focus was on revealing the relations between the honeycombs' mechanical properties as per their geometric configurations. From Table 4, it can be seen that among the honeycomb type NPTs, as the spoke cell angle θ decreases from 15.76 to 7°, the deformation of spokes decreases as well, meaning that HC-A3 has a higher load-carrying capacity than HC-A1. It is believed that the lower spoke cell angle results in a high amount of effective modulus in the radial direction, E_r/E_s [12]. The simple and trapezoid type NPTs have the least values of deformation, meaning that straight spoke structures have high load carrying ability than honeycomb-based NPTs and the pneumatic tyres [9]. The horizontal portions support the vertical spokes at 3 different points that provide a high amount of strength to the trapezoid structure and because of that, it has the least amount of flexibility/deformation than other spoke structures.

Table 4 Results of all types of NPTs under vertical load/force

Results	Force (N)	HC–A1	HC–A2	HC–A3	Simple spoke	Trapezoid	Pneumatic tyre [9]
Deformation of spokes (mm)	500	3.78	3.87	3.62	4	1.08	
Stress in spokes (MPa)		0.64	0.66	0.68	0.49	0.36	
Stress in tread (MPa)		0.216	0.2	0.21	0.21	0.2	
Strain energy spokes (mJ)		0.18	0.2	0.25	0.15	0.11	
Deformation of spokes (mm)	1000	7.26	7.43	7.2	7.28	3.93	5.78
Stress in spokes (MPa)		1.12	1.16	1.31	0.8	1.71	
Stress in tread (MPa)		0.29	0.29	0.28	0.31	0.27	
Strain energy spokes (mJ)		0.65	0.75	1.02	0.52	1.81	
Deformation of spokes (mm)	1500	9.96	9.91	10.1	10.56	7.05	
Stress in spokes (MPa)		1.55	1.66	1.67	1.25	2.28	
Stress in tread (MPa)		0.34	0.34	0.34	0.37	0.33	
Strain energy spokes (mJ)		1.24	1.57	1.81	1.29	3.18	
Deformation of spokes (mm)	2000	12.15	11.7	12.42	10.07	9.81	11.15
Stress in spokes (MPa)		1.93	2.13	2.14	1.62	2.86	
Stress in tread (MPa)		0.37	0.37	0.37	0.42	0.37	
Strain energy spokes (mJ)		1.89	2.57	3	2.18	5.02	
Deformation of spokes (mm)	2500	14.56	14.3	14.2	11.7	12.56	
Stress in spokes (MPa)		2.28	2.49	2.57	2.01	3.3	
Stress in tread (MPa)		0.39	0.39	0.39	0.45	0.39	
Strain energy spokes (mJ)		2.58	3.51	4.34	3.37	6.67	

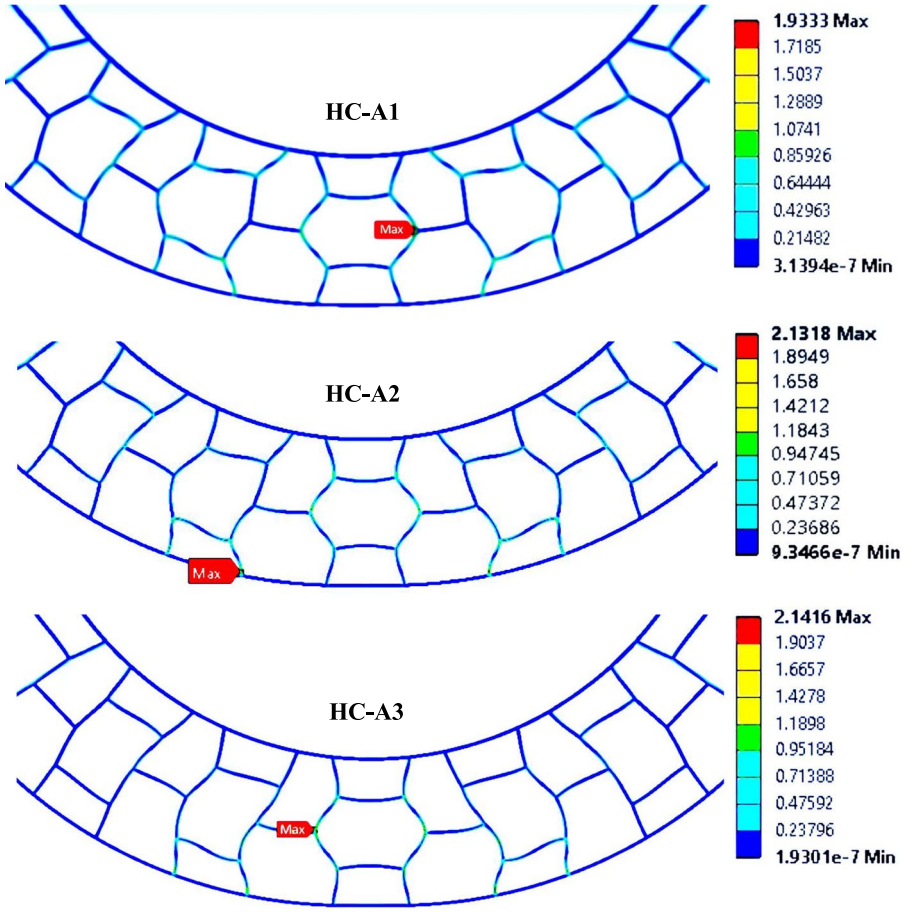

Fig. 10 Maximum spoke stresses (MPa) and deformation modes under 2000 N force

The lower local stresses and lower strain energy values in the spokes of the simple and HC-A1 structures are much better for the designing of the fatigue-resistant NPTs spokes. The trapezoid spoke structure can absorb the maximum amount of energy when deformed under vertical loading because it has the maximum value of strain energy, so it can be used in many of the energy absorbing structure applications.

Stress distribution results among the NPTs

In the simulation of NPTs, a point load was applied at the center of the hub ranging from 500 to 2500 N. The main focus of the number of stresses is in the spokes and the tread parts of the NPTs. Figure 10 shows the number of stresses and the deformation forms in the polyurethane spokes for the honeycomb type NPTs when at the hub center a force or load was applied of 2000 N. Elastic type of buckling can be seen in the deformed NPTs spokes. Stress concentration appears at the corner joint locations of cellular wall edges and the maximum stress for HC-A1, A2, and A3 are about 1.933, 2.132, and 2.141 MPa respectively at a load of 2000 N. The corner joints of spoke structures are weak areas and might fail first due to stress concentration. These corners must be filleted properly so that stress concentration is reduced, fatigue life, and

performance of the NPT is enhanced as well. The bottom half of the spoke structures undergo in bending or compression state while the top half is in the tension state and the stress is concentrated at the joint wall edges of the spokes. From the contours, it can be seen that among the honeycomb NPTs the HC-A3 has the highest amount of stress because of the lower cell angle of $\theta = 7^o$ and a radial modulus of elasticity value $E_r/E_s = 0.02$.

In Figs. 11 and 12, it is clearly shown that the stress in the spokes of NPTs gradually increases as the vertical force/load value is increased. In the graph of honeycomb spoke stresses, the least amount of stress is in the HC–A1, and the maximum amount of stress is in the HC–A3. So, as we reduce the value of cell angle θ of honeycomb spokes the amount of stress is increased. As per the above results, the honeycomb spoke structures have the potential in the design of sandwich structures due

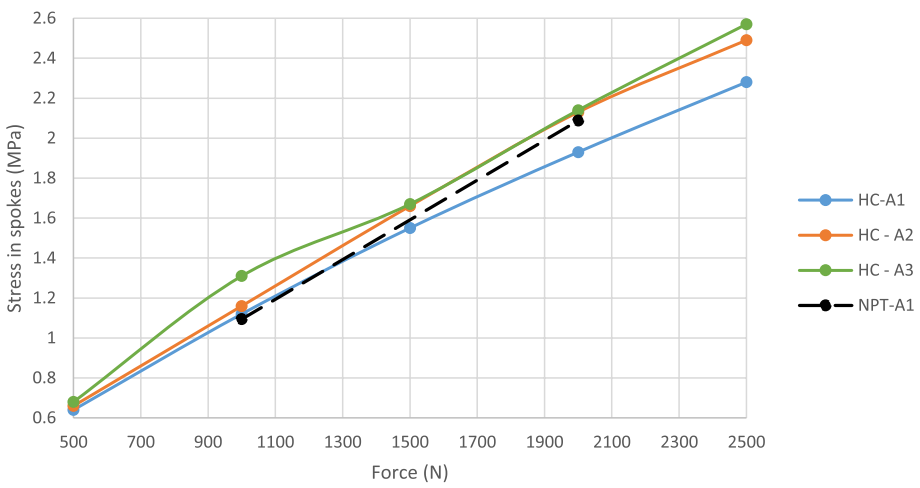

Fig. 11 Force (N) vs. maximum stress (MPa) graph for honeycomb spokes of NPTs [12]

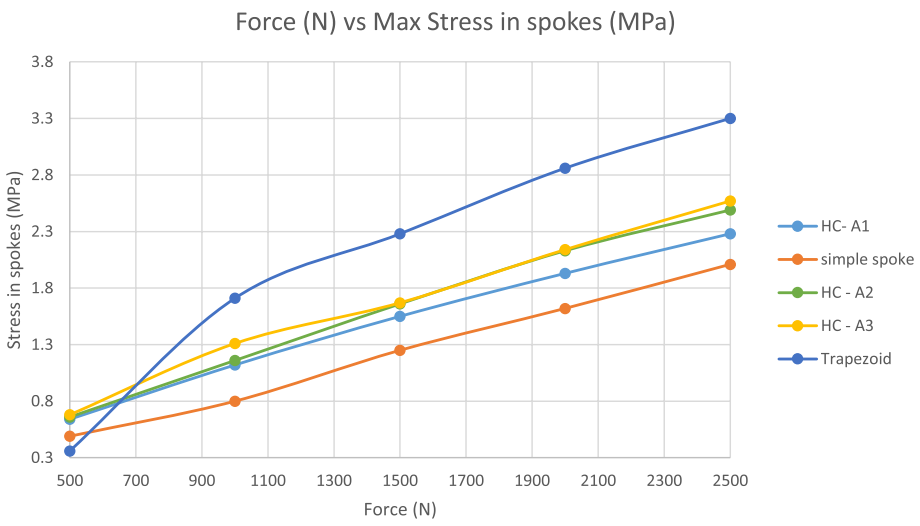

Fig. 12 Force (N) vs maximum stress (MPa) graph for spokes of NPTs

to their superior performance. From the results shown in Fig. 12, it can be seen that the stress is maximum in the trapezoid type NPT while the simple spoke type has the least amount of stress, it is because of the out of plane spoke structure design or lower cell angle spokes results in the high amount of stresses [4]. Table 5 shows the value of stress in spokes for the standard HC–A1 NPT and comparing it with NPT–A1 reference NPT [12], it is investigated numerically that the error between the HC–A1 and NPT–A1 design is minimum which shows that the simulation results are accurate. Considering the amount of maximum stress, the simple spoke and HC–A1 spoke structures are dominant over other structures. Because of the high amount of stress value in the spoke structure of trapezoid NPT, it has a low fatigue resistance, so simple spoke and HC-A1 design is given importance because of their low spoke stress values and high fatigue resistance.

Stress results in the tread of NPTs

The amount of stress between the flat platform and the tread is also observed. In Fig. 13, it is seen that as the force/load is applied, a rectangular shape contact is established on the tread's surface and this rectangular surface area increases as the force is increased. It is observed that along the lateral direction the contact pressure amount is steadier than along the circumferential direction. Figure 14 shows the stress in treads (MPa) of different NPT structures under vertical load/force. The maximum stress in the tread occurs in the simple spoke type structure because of the vertical spokes and no interconnectivity between the spokes. All the other spoke structures are interconnected with each other that is why the load is distributed equally between the spokes and the stress in the tread is almost the same for these structures.

Deformation results of NPTs spokes

The deformation of spokes or the load-carrying ability of NPTs is one of the main parameters in designing NPTs, which can be classified as the center of aluminum alloy hub displacement value. Figure 15 shows the deformation contours of all the straight spoke type NPTs under a vertical force of 2500 N. The straight spokes are acting just like columns and because of elastic buckling of spokes the maximum amount of deformation is at the center of the spokes equal to 12.56 mm and 11.702 mm for both the trapezoid and simple spoke NPTs as seen in Fig. 15. Among the honeycomb spokes, the HC–A3 has the least amount of deformation because the radial effective modulus E_r/E_s value of HC–A3 has the highest value of 0.02 because of the low cell wall angle of 7° [21]. This shows that among the honeycomb types, the HC–A3 has the highest load-carrying capacity and can be used as high load carrying structures in various other applications. Honeycomb spoke structures exhibit both structural integrity as well as efficient load

Table 5 Comparison of stress in spokes of HC–A1 and NPT–A1, NPTs [12]

Force (N)	Stress in spokes		% Error
	HC–A1	NPT–A1	
1000	1.12	1.094	2.32%
2000	1.93	2.088	7.57%

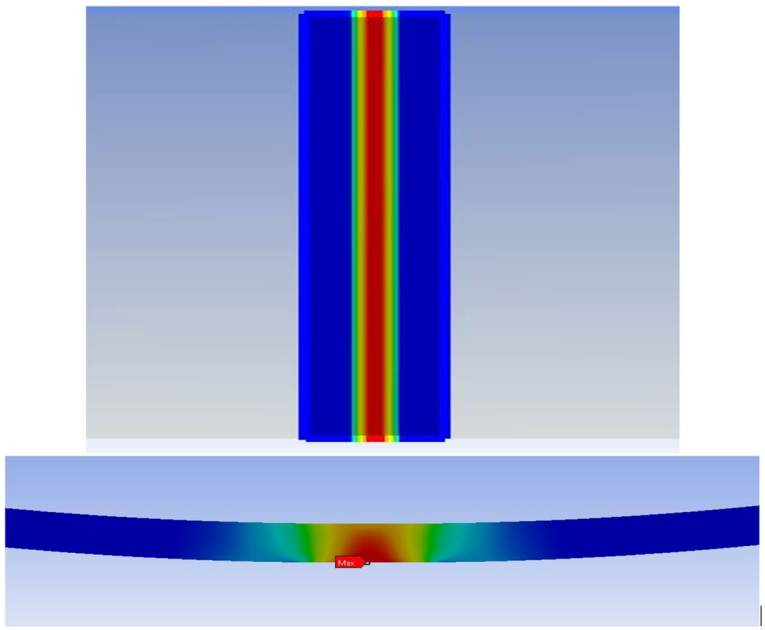

Fig. 13 Rectangular shape contact established between the tread and flat platform

distribution. While considering all the five types of NPTs, the simple spoke and the trapezoid one have the least amount of deformation as compared to the honeycomb structures. The straight-spoke NPTs have the highest amount of load-carrying ability, so they have more advantages over the other types and can be utilized in other applications like efficient load carrying structures that have low mass compared to other structures.

If we compare the deformation amounts of the simple spoke and trapezoid type NPTs with that of the pneumatic tyres, it is clear that the NPTs have a low amount

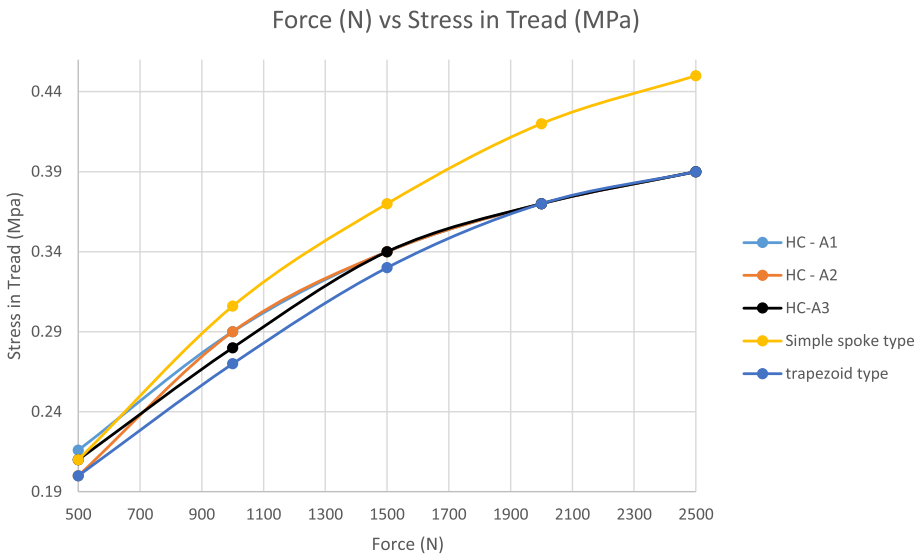

Fig. 14 Force (N) vs. stress in tread (MPa) graph for NPTs

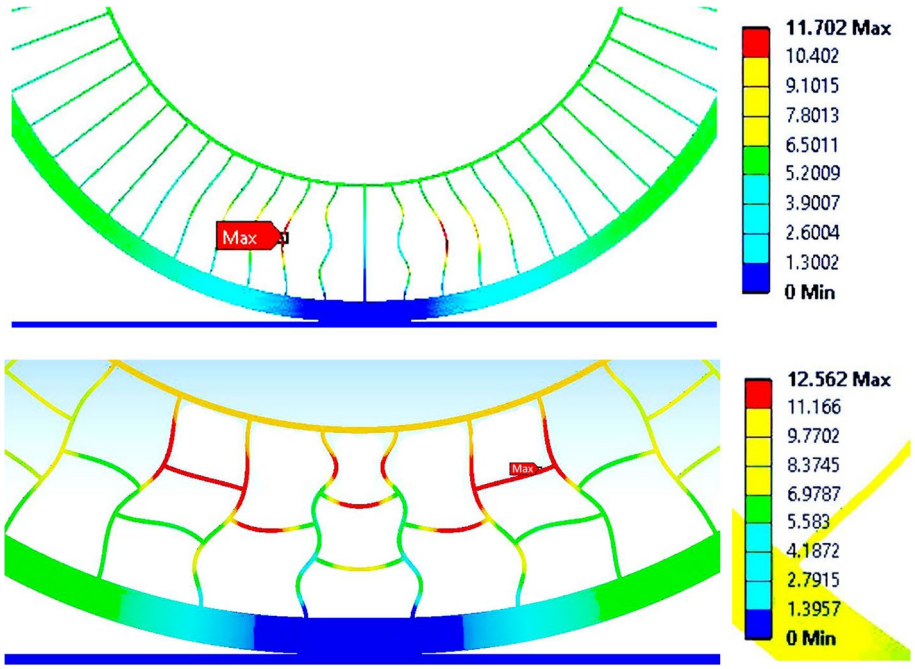

Fig. 15 Deformation contours at a force of 2500 N

of deformation and have a high load-carrying ability [9]. Now, this validates that our results are accurate and polyurethane material has a higher load-carrying ability than synthetic rubber material. Figure 16 shows a graph for all types of spoke structures against force (N) vs. the total deformation of spokes (mm). From the above results, the trapezoid type NPT is very suitable in high-load working environments because of its low amount of deformation.

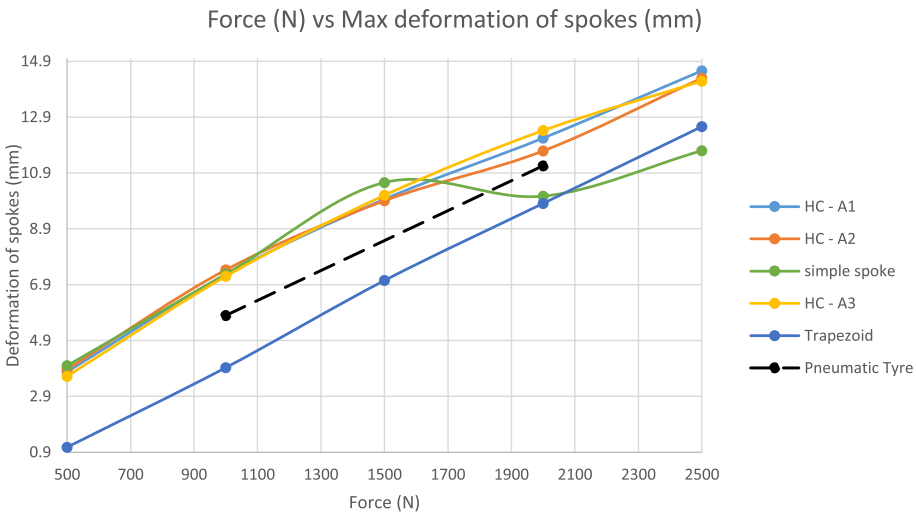

Fig. 16 Force (N) vs. max deformation of spoke structures (mm) graph for NPTs

Strain energy (mJ) results in spokes of NPTs

When a structure is under constant load, it has some amount of energy stored in it and when it is removed the energy that was stored is released just like in spring. This energy stored in a spoke structure within the elastic limit is called strain energy. If we consider a body that is under a force F, the cross-sectional area is A, length is L, and is deformed by an amount of Δ, so the work done W on the body is stored in it in the form of strain energy U [22].

$$W = \int F\, dL \tag{16}$$

$$U = \frac{1}{2}F\Delta = \frac{F^2L}{2EA} \tag{17}$$

Figure 17 shows that the maximum amount of strain energy is at the corner joint locations of the honeycomb spoke structures and the maximum values for HC-A1, A2, and A3 are about 2.578, 3.512, and 4.34 mJ under the load of 2500 N. If these corner areas are rounded off a bit, then the strain energy value around these areas will be distributed properly. From the contours, it is clear that among the honeycomb structures the HC–A3 has the highest amount of strain energy and it will absorb the maximum amount of energy when deformed under vertical loading. The effective radial

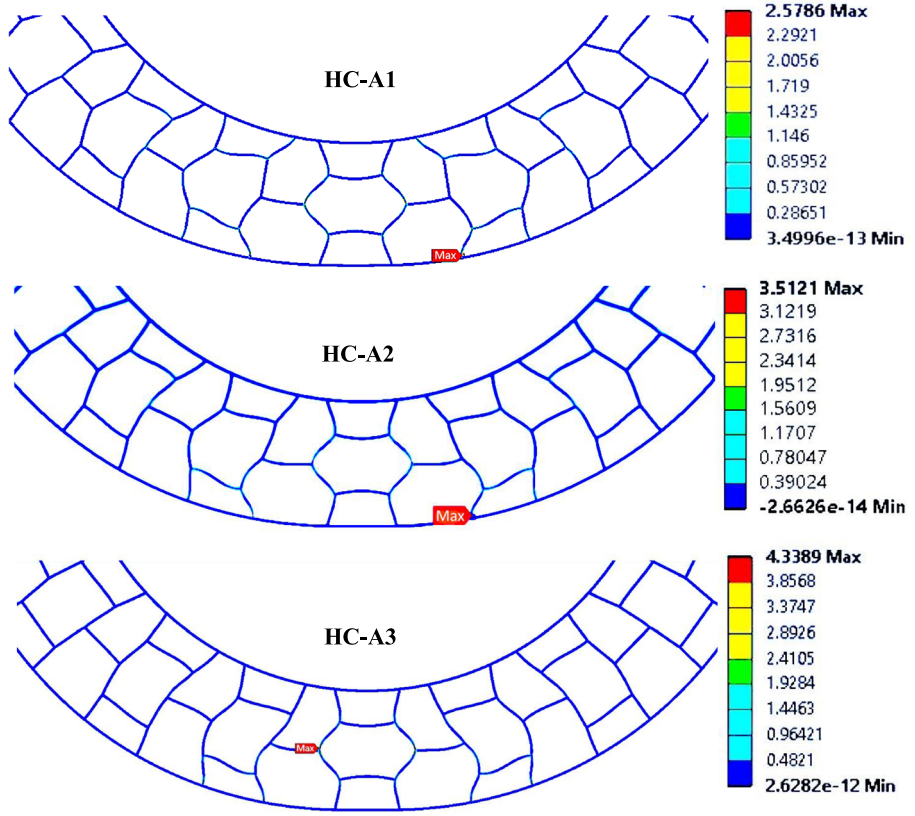

Fig. 17 Strain Energy (mJ) contours for the honeycomb NPTs at a force of 2500 N

modulus of elasticity $E_r/E_s = 0.02$, the value of HC–A3 is high, that is why it has a high value of strain energy (mJ).

It is proven that as the honeycomb cell angle θ value is decreased, the strain energy (mJ) of the structure increases. The trapezoid spoke structure has the highest value of strain energy (mJ) among all the other NPTs, so it will deform the least and will absorb all the loading energy. From the results, it can be concluded that as the strain energy value of a structure increases, the fatigue life of the structure decreases [23]. So for high fatigue life, NPT, and low load-carrying ability the HC–A1 is the best for such kinds of applications, and for high load carrying ability and a bit, less fatigue life than HC–A1 the simple spoke and trapezoid type NPTs are recommended. Figure 18 shows the graph between force (N) and strain energy in spokes (mJ) for all types of NPTs.

Conclusions

The static behavior of different types of NPT spoke structures was numerically analyzed using ANSYS MR-based nonlinear methods. The focus of this analysis is mainly on the total deformation and stress in the spoke structures, the stress in the treads of the NPTs, and also the strain energy in the spokes of NPTs. Five types of NPTs with the same wall thickness, with different geometric parameters, and having the same amount of mass were considered in the analysis. Now we can conclude our investigations as follows:

1. For the five types of NPTs designed with the same polyurethane wall thickness of 2 mm, the maximum amount of stress was found in the HC–A3 because of the lower cell angle, $\theta = 7°$ and the trapezoid straight spoke structure design. But the load-carrying ability of the simple spoke and the trapezoid type is the highest as compared to the honeycomb spoke designs, at 2500 N the values of the deformation are as follows 11.7 mm and 12.56 mm.
2. The stress in the tread of the simple spoke design has the highest value of 0.45 MPa at a load of 2500 N. This is because of the vertical spoke design and no intercon-

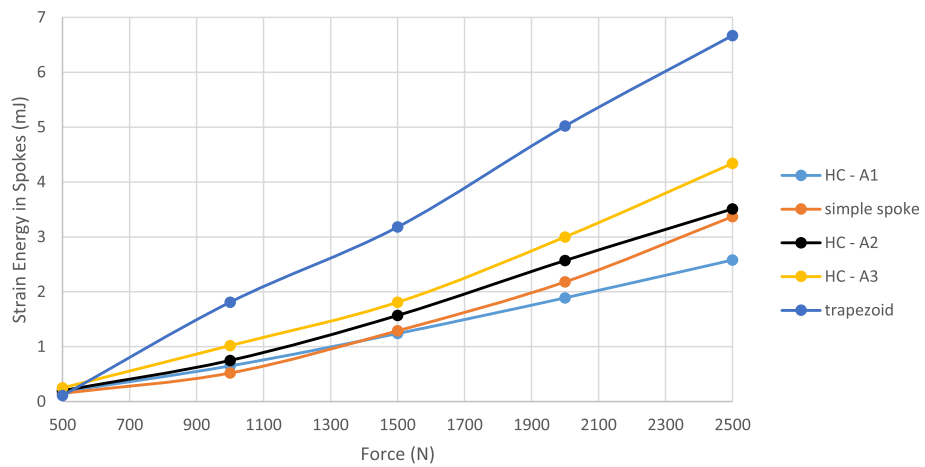

Fig. 18 Force (N) vs. strain energy in spokes (mJ) graph for NPTs

nectivity between the spokes. All the other spoke structures are interconnected with each other that is why the load is distributed equally among the spokes and the stress in the tread is almost the same for these structures equal to 0.39 MPa at a load of 2500 N.

3. The strain energy (mJ) in the spokes of the trapezoid design has the highest value of 6.67 mJ and HC–A1 has the lowest value of 2.58 mJ at a load of 2500 N, among the other types of NPTs. As the strain energy of the structure increases the fatigue life of the structure decreases. So for high fatigue life and low load-carrying ability the HC–A1 is the best for such kinds of applications and for high load carrying ability and less fatigue life than HC–A1 the simple spoke and trapezoid type NPTs are recommended.

Abbreviations

NPT: Non-pneumatic tyre; PU: Polyurethane; HC: Honeycomb; MPC: Multi-point constraints; FEA: Finite element analysis; CMT: Cellular materials theory; MR: Mooney-Rivlin.

Acknowledgements

The authors would like to acknowledge Ibrahim for his contribution as an expert guide and for assisting with the simulation part of this research. Also, we would like to thank all participants and experts for their participation in answering the preference questionnaire as well as being a member of the experts' panel.

Authors' contributions

M.A. as a 1st author wrote the paper, designed the different 2D tire spoke structures, analyzed the polyurethane spoke structures using ANSYS, and finally organized and compiled the results of the analysis. M.M. as a 2nd author helped M.A. to resolve the convergence issues in the non-linear analysis and guided all along the analysis part and also helped to compile the overall data of this research. Dr. A.H. Assistant Professor, Mechanical Engineering Department, UET TAXILA, supervised, guided, and helped to interpret and reviewed this paper as the main supervisor of this thesis. The authors have read and approved the final paper.

Funding

Not applicable. This study has no funding from any resource.

Availability of data and materials

The datasets used and/or analyzed during the current study are available from the corresponding author on reasonable request.

Declarations

Competing interests

The authors declare that they have no competing interests.

Received: 19 August 2021 Accepted: 30 March 2022
Published online: 12 April 2022

References

1. Rhyne TB, Cron SM (2006) Development of a non-pneumatic wheel. Tire Sci Technol 34(3):150–169. https://doi.org/10.2346/1.2345642
2. Cho JR, Kim KW, Yoo WS, Hong SI (2004) Mesh generation considering detailed tread blocks for reliable 3D tire analysis. Adv Eng Softw. 35(2):105–113. https://doi.org/10.1016/j.advengsoft.2003.10.002
3. "Energy Absorption of Structures and Materials - 1st Edition." https://www.elsevier.com/books/energy-absorption-of-structures-and-materials/lu/978-1-85573-688-7 (accessed 29 Jun 2021)
4. Sun Y, Wang B, Pugno N, Wang B, Ding Q (2015) In-plane stiffness of the anisotropic multifunctional hierarchical honeycombs. Compos Struct 131:616–624. https://doi.org/10.1016/j.compstruct.2015.06.020
5. Li Y, Abbès F, Hoang MP, Abbès B, Guo Y (2016) Analytical homogenization for in-plane shear, torsion and transverse shear of honeycomb core with skin and thickness effects. Compos Struct 140:453–462. https://doi.org/10.1016/j.compstruct.2016.01.007
6. Fan H, Jin F, Fang D (2009) Uniaxial local buckling strength of periodic lattice composites. Mater Des 30(10):4136–4145. https://doi.org/10.1016/j.matdes.2009.04.034

7. Ju J, Summers JD, Ziegert J, Fadel G (2010) Compliant hexagonal meso-structures having both high shear strength and high sehar strain. In: Proceedings of the ASME Design Engineering Technical Conference, vol 2, no. PARTS A AND B, pp 533–541. https://doi.org/10.1115/DETC2010-28672
8. Ju J, Summers JD (2011) Compliant hexagonal periodic lattice structures having both high shear strength and high shear strain. Mater Des 32(2):512–524. https://doi.org/10.1016/j.matdes.2010.08.029
9. Kim K, Kim DM, Ju J (2013) Static contact behaviors of a non-pneumatic tire with hexagonal lattice spokes. SAE Int J Passeng Cars Mech Syst 6(3):1518–1527. https://doi.org/10.4271/2013-01-9117
10. Ju J, Kim DM, Kim K (2012) Flexible cellular solid spokes of a non-pneumatic tire. Compos Struct 94(8):2285–2295. https://doi.org/10.1016/j.compstruct.2011.12.022
11. Ju J, Veeramurthy M, Summers JD, Thompson L (2013) Rolling resistance of a nonpneumatic tire having a porous elastomer composite shear band. Tire Sci Technol 41(3):154–173. https://doi.org/10.2346/tire.13.410303
12. Jin X, Hou C, Fan X, Sun Y, Lv J, Lu C (2018) Investigation on the static and dynamic behaviors of non-pneumatic tires with honeycomb spokes. Compos Struct 187(December 2017):27–35. https://doi.org/10.1016/j.compstruct.2017.12.044
13. Balawi S, Abot JL (2008) The effect of honeycomb relative density on its effective in-plane elastic moduli: an experimental study. Compos Struct. 84(4):293–299. https://doi.org/10.1016/j.compstruct.2007.08.009
14. Heo H, Ju J, Kim DM (2013) Compliant cellular structures: application to a passive morphing airfoil. Compos Struct. 106:560–569. https://doi.org/10.1016/j.compstruct.2013.07.013
15. Jin T, Zhou Z, Wang Z, Wu G, Shu X (2015) Experimental study on the effects of specimen in-plane size on the mechanical behavior of aluminum hexagonal honeycombs. Mater Sci Eng A 635(635):23–35. https://doi.org/10.1016/j.msea.2015.03.053
16. "material properties of polyurethane." http://www.matweb.com/search/DataSheet.aspx?MatGUID=26606798bc9d4538a7c7eadf78ab082b
17. Szurgott P, Jarzębski Ł (2019) Selection of a hyper-elastic material model—a case study for a polyurethane component. Lat Am J Solids Struct 16(5):1–16. https://doi.org/10.1590/1679-78255477
18. MSC. Software Corp (2010) Experimental elastomer analysis. User Guide, USA
19. "ANSYS mechanical structural non-linearities." https://studylib.net/doc/18120128/ansys-mechanical-ansys-mechanical-structural
20. Fatchurrohman N, Chia ST (2017) Performance of hybrid nano-micro reinforced mg metal matrix composites brake calliper: simulation approach. IOP Conf Ser Mater Sci Eng 257(1). https://doi.org/10.1088/1757-899X/257/1/012060
21. Fu MH, Chen Y, Hu LL (2017) A novel auxetic honeycomb with enhanced in-plane stiffness and buckling strength. Compos Struct. 160:574–585. https://doi.org/10.1016/j.compstruct.2016.10.090
22. Sadd MH (2014) 5.2 Elastic Strain Energy. Energy 3:123–125
23. Zhang J, Xue F, Wang Y, Zhang X, Han S (2018) Strain energy-based rubber fatigue life prediction under the influence of temperature. R Soc Open Sci 5(10):1–17. https://doi.org/10.1098/rsos.180951

Publisher's Note